# Automatic Joint Element Generation to Simulate Strain Softening Yield Behaviour in Earthern Materials

B. G. RICHARDS
Principal Research Scientist, Division of Soils, CSIRO

SUMMARY This paper describes a model incorporating automatically generated joint elements to simulate the observed behaviour of strain softening materials, including the post-yield behaviour. Good agreement was obtained when this model was used to back analyse triaxial and direct shear tests of such a material. The collapse load of strip footings as predicted by this model was also compared with previously published results, giving excellent agreement. This model, therefore has a useful capability of analysing the complete stress-strain behaviour of soils, including the prediction of the collapse load and the post-yield behaviour. At the same time, it maintains the advantages of non-linear elastic models in that it incorporates directly the constitutive relationships and the yield criteria based on experimental evidence, in this case, the results of conventional triaxial and direct shear tests.

## 1 INTRODUCTION

The stress-strain behaviour of naturally occurring soils is very complex and therefore difficult to simulate using mathematical models. Excellent summaries of such mathematical modelling techniques applicable to wide range of soil mechanics problems have already been given by numerous authors (e.g. Zienkiewicz et al., 1978). It is obvious that in the present state of understanding of soil behaviour and the definition of the relevent soil properties, accurate predictions of soil behaviour cannot be achieved. What is required for practical purposes, is to model as accurately as possible, those properties which are essential in the solution of a given problem. For this purpose, the finite element method has invariably been used with appropriate constituitive relationships for the stress-strain behaviour.

For pre-failure deformation states, non-linear elastic models have been developed to the point where they are the most suitable for the prediction of the stress-strain behaviour of soils so long as zones of near failure stress are limited. These models represent the soil as non-dilatant (i.e. shear stresses cause no volume change) with a non-associated behaviour (i.e. maximum shear strain occurs in the direction of the maximum shear stress). They also give poor simulation of the behaviour of soils which exhibit ideal plasticity or strain softening, but may prove adequate for those soils such as loose sands or normally consolidated clays, which exhibit continual strain hardening. Their main advantage is that they incorporate directly constituitive relationships based on experimental evidence e.g. the results of conventional triaxial compression tests with volume change measurements. This permits considerable flexibility in the use of the constituitive material relationships and for example permits the use of stress and/or strain dependent properties.

One such non-linear elastic model, which has been found to be simple to use in practical problems, is the hyperbolic stress-strain model, developed for clays by Konder (1963) and for sands by Konder and Zelasko (1963). Various forms of this model have subsequently been developed, but a modification of the Variable Moduli Model II (first proposed by Nelson, 1970) was used by the author (Richards, 1978) to model experimental stress-strain relationships for a range of soils in both field or laboratory applications. This model was shown to be able to describe the non-linear stress dependent properties of the soils based on the entire experimentally determined stress-strain curves at least, up to failure conditions.

For deformation states at or post-failure, most soil mechanics workers have extended the concepts of the classical plasticity theory to simulate the soil behaviour (Wroth, 1973). Whilst this theory applied only to ideal materials it had the advantage that the classical bounding theorems for collapse loads applied ensuring the uniqueness of the results. However, to obtain reasonable results with real soils, much of the classical theory had to be abandoned or considerably modified (Zienkiewicz et al., 1975).

The main problem with the classical plasticity theory was the assumption that the plasticity behaviour is "associated". It is now accepted (Davis, 1968a, 1968b; Davis and Booker, 1973; Zienkiewicz et al., 1975) that associated behaviour using Mohr-Coulomb yield criteria contradicted experimental observations and gave excessive rates of dilation. Attempts to extend plasticity ideas to a "non-associated" form have become necessary, but no useful bounds can be placed on the collapse loads and this creates doubts on the uniqueness of the results. Consequently, one of the main advantages of the plasticity theory no longer applies.

This paper looks at the possibility of extending the hyperbolic stress-strain model to simulate the failure and post-failure behaviour of strain softening soils. In one application (Richards, 1979) viz. the back-analyses of spoil pile failures at a strip coal mine in the Bowen Basin, Queensland, strain softening of the spoil pile was the significant factor. As no other method of analysis was found to be suitable, the finite element program using the hyperbolic stress-strain model was modified to include fixed joint elements (Ghaboussi et al., 1973) along the previously surveyed location of the failure planes. These joint elements had non-linear hyperbolic shear

stress-displacement relationships with a shear stress release and redistribution technique to simulate strain softening (Zienkiewicz et al., 1968; Lo and Lee, 1973). Using the elastic properties from triaxial tests and joint properties from direct shear tests, it was possible to closely model both the triaxial and shear box tests themselves as well as the slope behaviour in the field.

One interesting point arising out of the analyses of the spoil piles was the fact that the maximum shear strain contours given by the non-linear elastic analyses predicted the location of the observed failure planes very closely as suggested by Resendiz and Romo (1972). This led to the possibility of inserting joint elements automatically into the finite element mesh when yield occurs, at the location and orientation determined by the yield criteria adopted.

## 2 MATERIAL MODEL

### 2.1 Basic Continuum Model

The hyperbolic model used to describe the continuum material up to yield can be summarized by the simplified relationships (Richards, 1978) as:

$$K = K_1 \sigma_m^{\ n} + K_o \qquad (1)$$

and

$$G = G_1 \sigma_m^{\ m} \left(1 - \left(\frac{\tau}{\tau_f}\right)^p\right) + G_o \qquad (2)$$

where $K$ = bulk modulus
$G$ = shear modulus
$\sigma_m$ = maximum value of the mean stress
$= 1/3\ (\sigma_1 + \sigma_2 + \sigma_3)$
$\sigma$ = shear stress) according to yield
$\sigma_f$ = yield stress) criteria adopted

$K_1$, $K_o$, $G_1$, $G_o$, $n$, $m$ and $p$ are material constants.

These equations can readily be programmed into non-linear elastic finite element programs using continuum elements and incremental loading. Typical results using such a program have already been published elsewhere (Richards, 1978).

### 2.2 Joint Elements

The joint element used in the finite was based on that proposed by Ghaboussi et al., (1973). The finite element formulations for constant strain joint elements are:

$$\{F_n\} = [k]\ \{\sigma_n\} \qquad (3)$$

where $[k]$ = stiffness matrix
$k_{ns} = \int vol\ B^T C\ B dvol.$
$[C]$ = stress matrix
$[B]$ = strain matrix
$\{F_n\}$ = nodal forces
$\{\sigma_n\}$ = nodal displacements

The strain matrix $[B]$ as used by Ghoboussi et al., (1973) is similar in form to that for the simple constant strain continuum elements. However, the stress matrix $[C]$ is different and has the form for two dimensional problems:

$$\begin{matrix}\sigma_n \\ \sigma_t \\ \sigma_s\end{matrix} \begin{bmatrix} C_{nn} & 0 & C_{ns} \\ 0 & 0 & 0 \\ C_{sn} & 0 & C_{ss} \end{bmatrix} \begin{matrix}\varepsilon_n \\ \varepsilon_t \\ \varepsilon_s\end{matrix} \qquad (4)$$

where $\sigma_n$ = stress normal to joint
$\sigma_t$ = stress transverse to joint
$\sigma_s$ = shear stress in joint direction
$\varepsilon_n$ = strain normal to joint
$\varepsilon_t$ = strain transverse to joint
$\varepsilon_s$ = shear strain in joint direction

$C_{nn}$, $C_{ns}$, $C_{sn}$ and $C_{ss}$ are the joint parameters
$C_{nn}$ = joint stiffness normal to joint
$C_{ss}$ = shear stiffness of joint
$C_{ns} = C_{sn}$ is the coupling between normal displacement and shear force and vice-versa (i.e. are zero for non-dilatant joints).

Thus it can be seen that any continuum element can be converted to an effective joint element by changing the stress matrix $(D)$ for a continuum element to the $(C)$ matrix for a joint element at any time when yield occurs during the incremental loading process. This technique has been checked by comparing analyses with those using the specially designated joint elements as defined by Ghaboussi et al., (1973). The joint parameters differ from the elastic parameters, but in the following examples, $C_{nn}$ has been equated with $3K$ and $C_{ss}$ with $G$ with $C_{ns}$ and $C_{sn}$ equal to zero (i.e. equivalent to putting $\nu = 0$).

The main difficulty in changing to the joint element is the determination of the joint angle, $\alpha$, i.e. the angle between the n-s co-ordinate system of the joint and the x-y co-ordinate system used in the analysis. Morgenstern and Tchalenko (1967) have investigated the microscopic structures in kaolin subjected to direct shear and considered two component viz. original fabric (e.g. pre-existing joints) and shear-induced fabric (e.g. joints formed during the loading stages). Up to failure i.e. the creation of a discontinuity or a joint, the deformations are assumed to be strain controlled, but the formation of the joint is due to a displacement discontinuity and the deformations are the result of principle displacement shear (Skempton, 1966). Hence the best estimate of the angle $\alpha$, at least for a non dilatant material, is given by the maximum or principal shear strain direction corresponding to the incremental nodal displacements during yield i.e. joint formation.

The stiffness matrix for the joint element in the general x-y co-ordinate system is:

$$[k]_{xy} = [T]^T [k]_{ns} [T] \qquad (5)$$

where $[T]$ is the transformation matrix containing the direction cosines of the joint angle, $\alpha$.

### 2.3 Strain Softening

The model used in this paper assumes that strain softening occurs only in the joint elements. At yield, the actual shear stresses are equal to or exceed the yield stresses for peak strength and the shear stiffness from equation (2) has been reduced to near zero values. The yield stresses for residual strength are then calculated and the difference is redistributed until the shear stresses in the yielded elements are at the residual values.

The excess shear stress along the joint at angle, $\alpha$, is given by:

$$\Delta\tau_\alpha = \tau_\alpha - \tau_{\alpha R} \qquad (6)$$

where $\tau_\alpha$ = actual shear stress along the joint
$\tau_{\alpha R}$ = residual shear strength

The excess stresses to be redistributed in the x-y co-ordinate system are given by:

$$\{\Delta\sigma\} = \begin{Bmatrix} \Delta\sigma_x \\ \Delta\sigma_y \\ \Delta\tau_{xy} \end{Bmatrix} = \begin{Bmatrix} -\Delta\tau_\alpha \sin 2_\alpha \\ \Delta\tau_\alpha \sin 2_\alpha \\ -\Delta\tau_\alpha \cos 2_\alpha \end{Bmatrix} \qquad (7)$$

where $\alpha$ is the inclination of the joint to the horizontal.

Using the "initial stress" method (Zienkiewicz et al., 1968), the excess stresses are redistributed by generating a new set of nodal forces.

$$\{F\} = \int (B)^T \{-\Delta\sigma\} \, dvol \qquad (8)$$

where $(B)^T$ is the transpose of the strain matrix

$\{-\Delta\sigma\}$ is the negative value of the excess stresses

As the shear modulus of the yielded elements is near zero, the iterative method used by Lo and Lee (1973) was not required for the reduction of the stresses in the yielded elements, but was required to ensure redistribution of these stresses to the elements not yet yielded.

## 2.4 Tensile Failure

The model used for tensile failure in some of the applications described in the following sections was simply to reduce any tensile stresses exceeding the tensile strength of the material to zero and redistribute them by the "initial stress" method discussed above.

# 3 ANALYSES OF LABORATORY TESTS

The mud stone underlying the coal and forming the floor of a strip coal mine in the Bowen Basin, Queensland has already been extensively investigated (Richards, 1979). This material exhibited brittle failure with strain softening and little or no volume change or dilatancy. It was therefore an ideal material for the application of the model described above. This material also formed the base of the spoil piles, standing over 70 metres high at their natural angle of repose (up to 35°) and which have had a history of failures (Boyd et al., 1978).

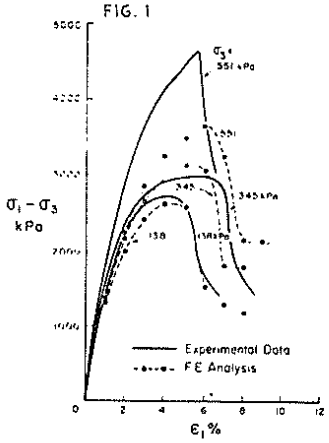


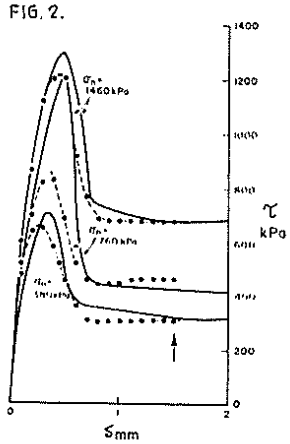


*Figure 1. Triaxial test results for mud-stone, Bowen Basin, Queensland.*

*Figure 2. Direct shear test results for mud-stone, Bowen Basin, Queensland: Shear stress versus shear displacement.*

Undrained triaxial tests without volume change measurement were carried out on 200 mm dia. sealed 'intact' cores of the material sampled at its natural water content. Typical results of the deviatoric stress versus vertical strain curves for various cell pressures are shown in Fig. 1. Direct shear tests were also carried out on the same material and typical shear stress versus displacement curves for various normal stresses are shown in Fig. 2. The normal displacement versus shear displacement curves for the same samples is shown in Fig. 3.

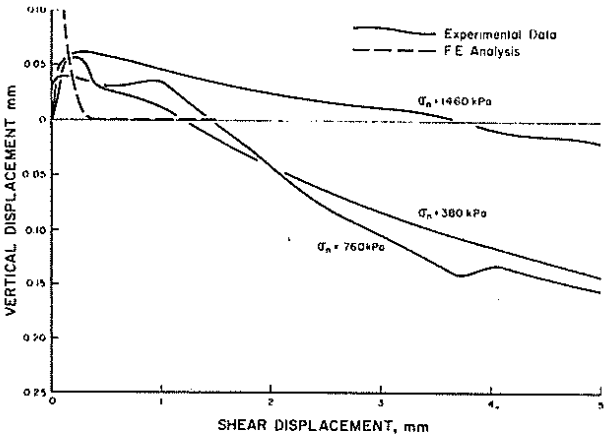


*Figure 3. Direct shear test results for mud-stone, Bowen Basin, Queensland: Normal displacement versus shear displacement.*

The hyperbolic parameters including the peak strength parameters as defined in equations (1) and (2) were determined using the triaxial data in Fig. 1. The residual strength parameters were determined using the direct shear box data in Fig. 2. These parameters can be summarized in the following expressions:

$$K = 154{,}000 \text{ kPa}$$

$$G = 71{,}000 \left(1-\left(\frac{\tau}{\tau_f}\right)^{1.0}\right) + 150 \text{ kPa}$$

$$C_{nn} = 462{,}000 \text{ kPa}$$

$$C_{ss} = G$$

$$C_{ns} = C_{sn} = 0$$

$\tau_{fp}$ = peak yield stress, $(\sigma_1-\sigma_3)_p/2$

$$= 625 \cos 34^o + (\sigma_1+\sigma_3) \sin 34^o \text{kPa}$$

$\tau_{fr}$ = residual yield stress

$$= 170 + \sigma_n \tan 16^o \text{ kPa}$$

It should be noted that the triaxial test using Mohr-Coulomb yield criteria and the direct shear test using the Coulomb criteria on the failure plane give different results for non-associated materials (Davis, 1968b and Morgenstern et al., 1967). This difference is taken into account in the model described above as the shear strength on the actual failure plane is predicted not assumed in each analysis.

The laboratory tests showed that the material exhibited little or no dependency on the mean stress and soil suction. For example, the effect of soil suction on the residual shear strength is shown in Fig. 4.

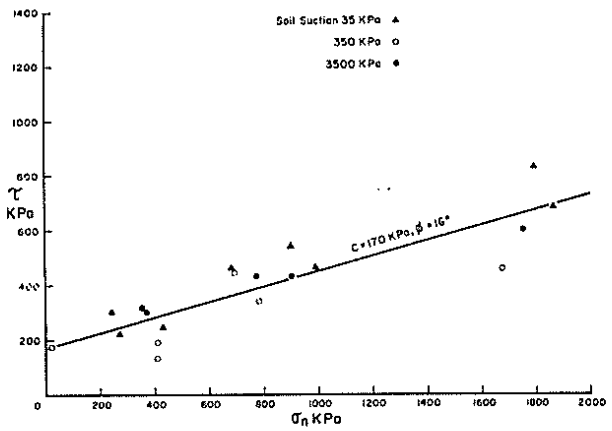


*Figure 4. Direct shear test results for mud-stone, Bowen Basin, Queensland: Residual shear strength versus soil suction.*

Using these parameters, the laboratory tests themselves were back-analysed. The triaxial tests could not be exactly modelled as the applied stresses were axi-symmetric, but the observed failure planes were distinct planar surfaces at angles of 50° to 55° to the horizontal. As a compromise, the triaxial tests were modelled as plane strain tests as these give planar failure surfaces similar to those observed and the intermediate stress, $\sigma_2$, does not affect the Mohr-Coulomb yield criteria. The results of these plane strain analyses are summarized in Figs. 1, 5, 6 and 7 and gave excellent agreement with the test data.

Similar plane strain analyses of the direct shear tests were carried out assuming a shear plane 2 mm thick. The results of these analyses are summarised in Figs. 2, 8 and 9. It is interesting that the directions of the maximum shear strains varied from 25° to the horizontal initially to approximately 0° at yield. Therefore, any shear induced sub-structures could be similar to those reported by Morgenstern and Tchalenko (1967).

One obvious question, which could be raised concerning these analyses, is the influence of the finite element mesh, particularly the orientation of the nodes in the simulated triaxial tests as shown in Fig. 10. Analyses were repeated of these tests with no strain softening (i.e. $\tau_{fp} = \tau_{fr}$), but with the orientation of the nodes varied. Fig. 10 also shows the stress-strain results for a 45° orientation and Fig. 11 shows the variation of predicted peak strength with node orientation. In each case, the joint angles, $\alpha$ at yield were predicted to be approximately 52° in the vicinity of the failure surface, which corresponded with the angle for minimum strength shown in Fig. 11. The failure surfaces predicted by the maximum shear strain contours were stepped except in the case of the nodes orientated at 52°, but in each case, the average slope approximated 52°. At an orientation greater than 63°, every diagonal line of nodes was impeded by the end caps and this apparently impeded failure as shown in Fig. 11.

## 4 ANALYSES OF THE YIELDING OF STRIP FOOTINGS

The first example analysed was that of a rigid frictionless strip footing being pushed into weightless frictionless soil at a constant strain rate. Fig. 12 shows the geometry of the problem and Fig. 13 the displacement (i.e. flow) patterns at peak load. Fig. 12 also shows the load-settlement curve, which compares favourable with the Prandtl solution. Results for a similar analysis with strain softening such that $\tau_{fr} = 0.5\tau_{fp}$ is also shown in Fig. 12.

Attempts at analysing a cohesionless soil were not so successful as convergence could only be achieved after a very large number of iterations per increment of loading. While the initial stress method used ultimately gives the correct result, intermediate results can give temporary peak strengths much higher than the true peak strength.

As a further check on the model, the plane strain analysis of a uniformly loaded flexible and frictionless strip footing by Zienkiewicz et al., (1975) was repeated. The load settlement curve is shown in Fig. 17 compared with their curve for non-associated flow (θ=0) and the Prandtl collapse load. The differences between the load-settlement

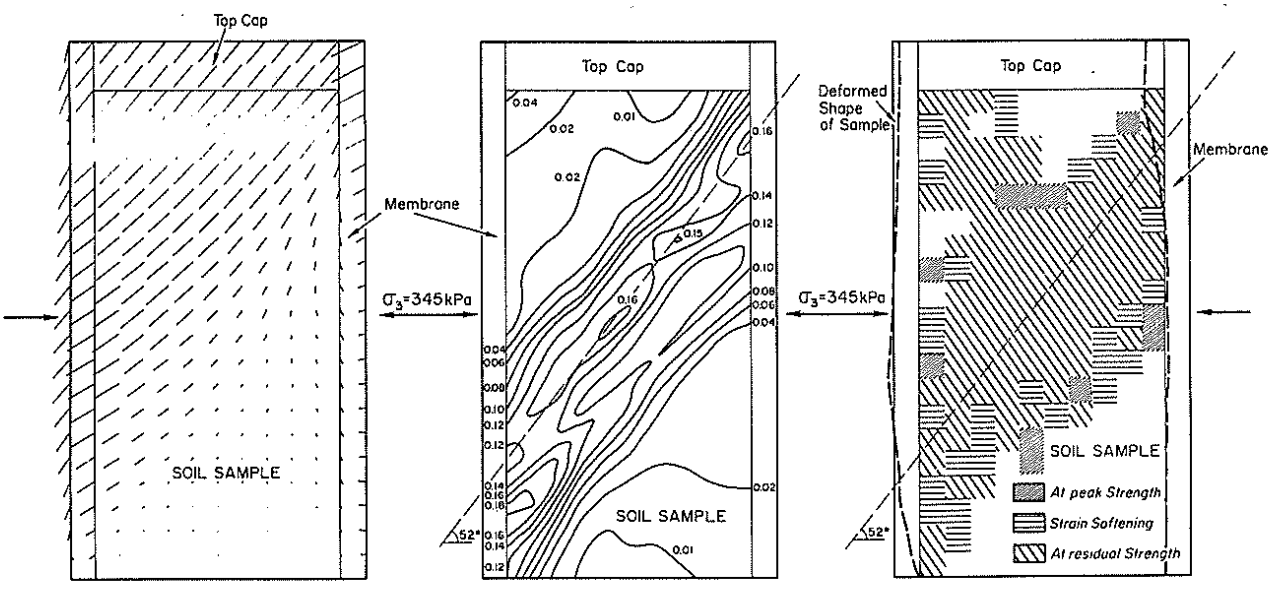


FIG.5 FIG.6 FIG.7

*Figure 5. Results of finite element analysis of triaxial test: displacement vectors.*
*Figure 6. Results of finite element analysis of triaxial test: max. shear strain contours.*
*Figure 7. Results of finite element analysis of triaxial test: zones of failure.*

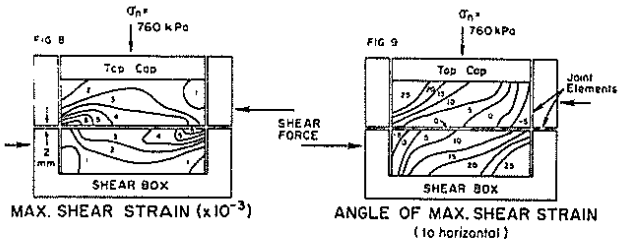


*Figure 8. Results of finite element analysis of direct shear test: max. shear strain contours.*
*Figure 9. Results of finite element analysis of direct shear test: orientation of joint angles.*

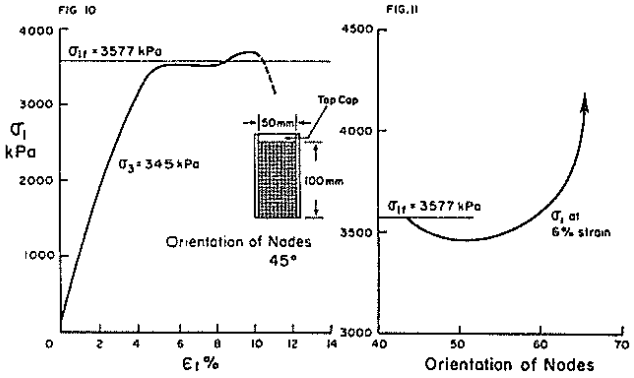


*Figure 10. Results of finite element analysis of plane strain test with elements at 45° orientation.*
*Figure 11. Variation of predicted shear strength with element orientation.*

curves in Fig. 17 are due to the differences between the linear elasticity used by Zienkiewicz et al. and the non-linear elasticity used in this paper. The displacement patterns post-yield are shown in Fig. 15. Figs. 16 and 17 show the maximum shear strain contours and the spread of yielded zones at peak load.

## 5 ANALYSES OF SLOPE FAILURES

Space does not permit a detailed description of the analyses of slope stability problems. However, the analyses of a spoil failure at the Goonyella mine, Queensland, previously reported by the author (Richards, 1979) were repeated using the model described above with very similar results. Using the construction sequence shown by stages 1 to 6 and the final rise in the groundwater level, i.e. stage 7 shown in Fig. 18 together with the actual material parameters previously determined, the analyses indicated that the slope was near failure. The displacement pattern shown in Fig. 19 and yielded zones shown in Fig. 20 indicate that the predicted failure planes

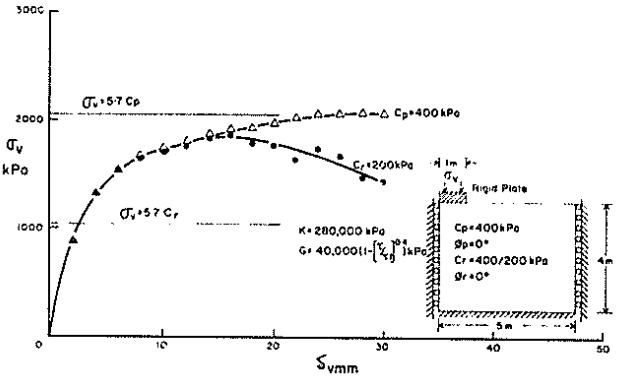


*Figure 12. Load-settlement curve for rigid frictionless strip footing.*

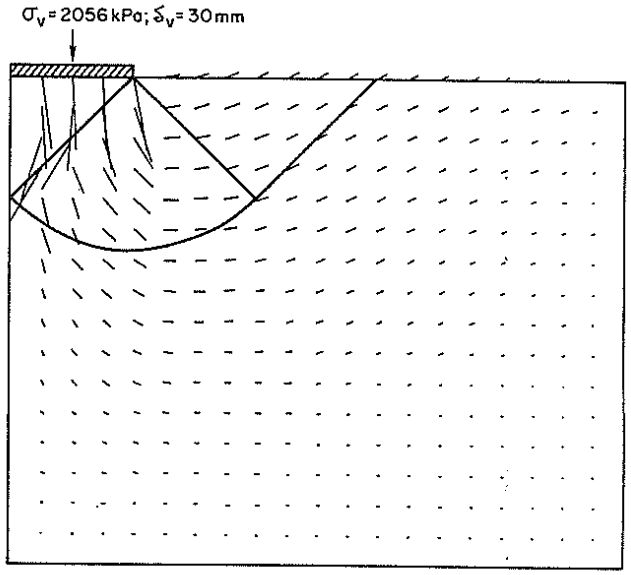


*Figure 13. Displacement vectors for rigid frictionless strip footing at yield.*

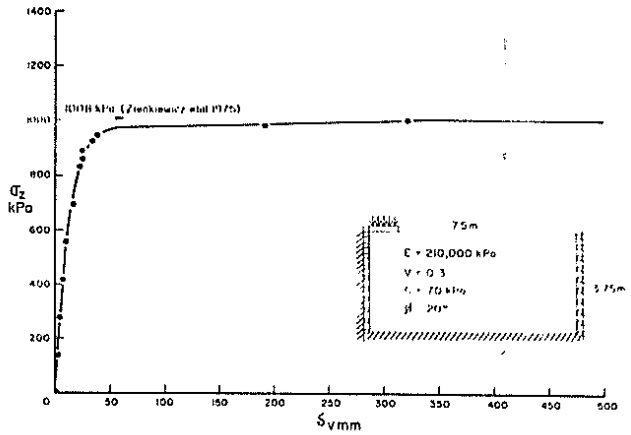


*Figure 14. Load-settlement curve for flexible frictionless strip footing.*

would be similar to those observed and used in the previously reported analyses.

## 6 CONCLUSIONS

The model incorporating automatically generated joint elements as described in this paper has been used to closely simulate the observed behaviour of a strain softening material including the post-yield behaviour in laboratory tests. Results for the collapse load of strip footings also compare favourably with those obtained previously using visco-plasticity models and the Prandtl collapse loads. Attempts at modelling the strain softening effects in a spoil pile at a strip coal mine were successful and predicted the sequential failure a manner similar to that observed in an actual failure.

This model therefore has a useful capability of analysing the complete stress-strain behaviour of soils including the prediction of the collapse load and the post-yield behaviour. At the same time, it maintains the advantages of non-linear elastic models in that it incorporates directly the constitutive relationships and yield criteria based on experimental evidence, in this case, the results of conventional triaxial and direct shear tests.

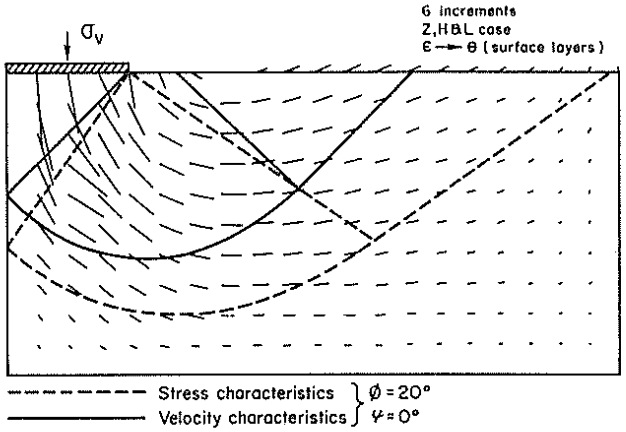


*Figure 15. Displacement vectors for flexible frictionless strip footing.*

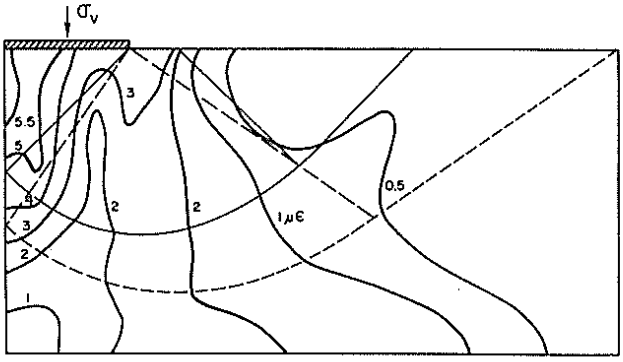


MAX. SHEAR STRAIN

*Figure 16. Contours of max. shear strain for flexible frictionless strip footing.*

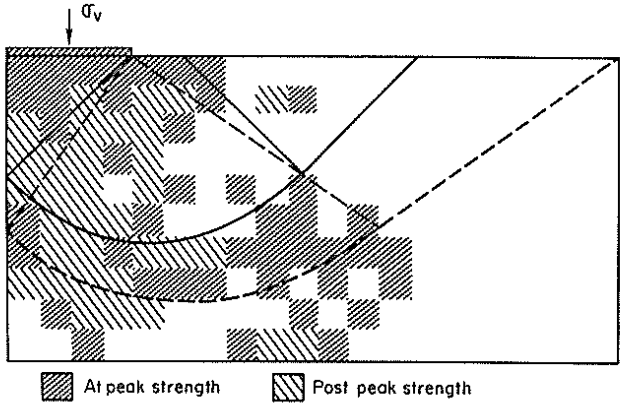


*Figure 17. Zones of failure for flexible frictionless strip footing.*

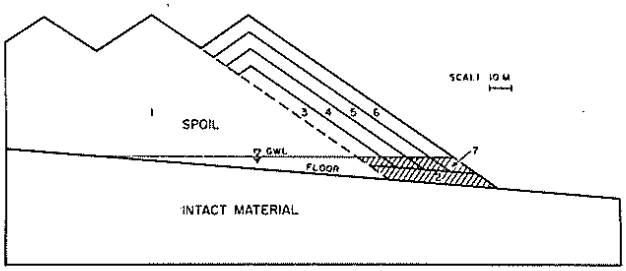


*Figure 18. Construction sequence for spoil pile.*

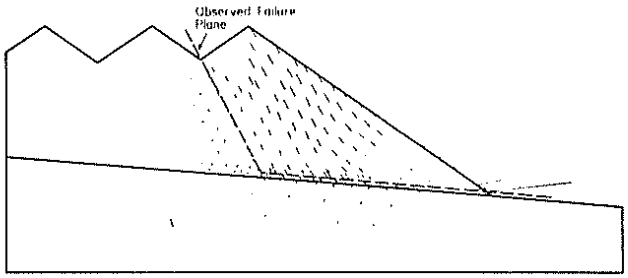


*Figure 19. Displacement vectors for completed spoil pile.*

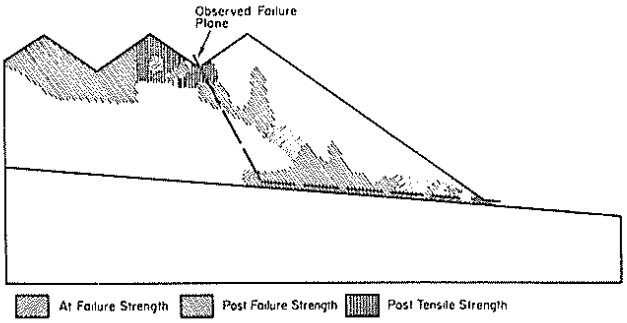


*Figure 20. Zones of failure for completed spoil pile.*

## 7 REFERENCES


ZIENKIEWICZ, O.C., NORRIS, V.A., WINNICKI, L.A., NAYLOR, D.J. and LEWIS, R.W. (1978). A Unified Approach to the Soil Mechanics Problems of Offshore Foundations, in "Numerical Methods in Offshore Engineering" ed. by O.C. Zienkiewicz, R.W. Lewis and K.G. Stagg, Chicester, Wiley, 1978.

KONDER, R.L. (1963). Hyperbolic Stress-Strain Response: Cohesive Soils, J. Soil Mech. and Foundations, Div., A.S.C.E., Vol. 89 No. SMI, pp 115-143.

KONDER, R.L. and ZELASKO, J.S. (1963). A Hyperbolic Stress-Strain Formulation for Sand. Proc. 2nd Pan-American Conf. on Soil Mech. and Fndn. Engng., Vol. 1, pp 289-333.

NELSON, I. (1970). Investigation of Ground Shock Effects in Non-linear Hysteretic Media. Report 2, Modelling the Behaviour of a Real Soil, Report S-68-1, Contract DACA 39-67-C-0048, Paul Weidlinger Consulting Engineer, U.S. Army Waterways Experiment Station.

RICHARDS, B.G. (1978). Application of an Experimentally Based Non-linear Constitutive Model of Soils in Laboratory and Field Tests. Aust. Geomechanics Journal, Vol. G8, pp 20-30.

WROTH, C.P. (1973). A Brief Review of the Application of Plasticity to Soil Mechanics Proc. Symp. Role Plasticity in Soil Mech., Cambridge, 1-11 (ed. A.C. Palmer).

ZIENKIEWICZ, O.C., HUMPHESON, C. and LEWIS, R.W. (1975). Associated and Non-associated Visco-plasticity and Plasticity in Soil Mechanics, Geotechnique, 25(4):671-689.

DAVIS, E.H. (1968a). A Discussion of Theories of Plasticity and Limit Analysis in relation to the failure of soil masses. Proc. 5th Aust. N.Z. Conf. Soil Mech. and Fndn. Engng. 175-182.

DAVIS, E.H. (1968b). Theories of Plasticity and the Failure of Soil Masses. In "Soil Mechanics: Selected Topics" (Ed. I.K. Lee): 341-380, London, Butterworths.

DAVIS, E.H. and BOOKER, J.R. (1973). Some Applications of Classical Plasticity Theory for Soil Stability Preblems. Plasticity and Soil Mechanics, Cambridge, 24-43.

RICHARDS, B.G. (1979). Finite Element Analyses of Spoil Pile Failures at the Goonyella Mine, CSIRO, Div. of Appl. Geomech., Tech. Report No. 96.

GHABOUSSI, J., WILSON, E.L., and ISENBERG, J. (1973). Finite Element for Rock Joints and Interfaces, Proc. ASCE, Jn. Soil Mech. and Fndn. Div., 99 (SMIO):833-848.

ZIENKIEWICZ, O.C., VALLIAPAN, S. and KING, I.P., (1968). Stress Analysis of Rock, as a "No-tension" material, Geotechnique, 18(1):56-66.

LO, K.Y. and LEE, C.F. (1973). Stress Analysis and Slope Stability in Strain-softening Materials, Geotechnique, 23(1):1-11.

RESENDIZ, D. and ROMO, M.P. (1972). Analysis of Embankment Deformations Proc. ASCE, Specialty Conf. on Performance of Earth and Earth Supported Structures, Purdue University, Vol. 1, Part 1:817-836.

MORGENSTERN, N.R. and TCHALENKO, J.S. (1967). Microscopic Structures in Kaolin Subjected to Direct Shear, Geotechnique, 17(4):309-382.

SKEMPTON, A.W. (1966). Some Observations on Tectonic Shear Zones, Proc.
BOYD, G.L., KOMDEUR, W. and RICHARDS, B.G. (1978). Open Strip Pitwall Instability at Goonyella Mine - Causes and Effects, Aust. I.M.M. Conf., North Queensland, :139-157.